

# Determination of Heat Transfer Coefficient for the Air Forced Cooling Over a Flat Side of Coil

Payam Shams Ghahfarokhi\* (*Researcher, Tallinn University of Technology, Tallinn, Estonia*),  
Ants Kallaste (*Senior Researcher, Tallinn University of Technology, Tallinn, Estonia*),  
Anouar Belahcen (*Professor, Aalto University, Espoo, Finland*),  
Toomas Vaimann (*Senior Researcher, Tallinn University of Technology, Tallinn, Estonia*)

**Abstract** – The paper deals with the analytical and experimental determination of the forced convection heat transfer coefficients over the flat coil module. In the analytical part, the forced convection coefficients at different wind speeds are calculated based on various known equations of the forced convection heat transfer coefficient with unheated starting length. The experimental part presents the description of the test: loading the coil with DC current and measurements of the coil temperatures with thermal sensors while it was inside a wind tunnel. Based on the measurement, the convection coefficients were determined. In the final part, the experimental and analytical results are compared. It is found that the accuracy of the analytical results is more precise in highly turbulent flows.

**Keywords** – Flat surface; Forced convection; Heat transfer coefficient; Laminar and turbulent flow.

## I. INTRODUCTION

Along with the significant progress in the electronic and electric industries, the electronic and electrical devices become routine facilities of the daily life of human beings [1], [2]. Due to high competition in the strife to manufacture ever more economical products, minimizing the size and weight of the products is essential [2]. However, reducing the size of the device, the amount of heat flux per volume of the device is increasing significantly [2]. Accordingly, to provide a reliable operation temperature during the working conditions for these devices, thermal design and analysis are of great importance and play a vital role in the design process.

Heat is transferred from the object to the ambient by three phenomena: conduction, convection and radiation [3]. A significant part of heat is transferred by the phenomenon of convection, which may be of two types: natural and forced convection [4]. The amount of heat transferred from the object's surface to the ambient is proportional to the velocity of fluid flow [5]. In natural convection, the speed of fluid flow is very low. Thus, the amount of heat transfer from the surface to the ambient is small, as a result, the value of the convection coefficient is low [5]. Accordingly, the natural cooling method is used in low power electronic and electric devices. To increase the amount of transferred heat by convection, the velocity of the fluid flow should be increased [5]. For this purpose, the forced cooling methods are implemented in different electric and electronic devices to increase the

velocity of the fluid flow, which leads to higher convection coefficient. There are several different forced cooling methods [6]. Implementing a distinct cooling system is one of the effective forced cooling methods for increasing the fluid motion. A wind tunnel technology is one of the common distinct cooling methods that can be applied instead of extra equipment in the devices for increasing the coolant speed. This technology is located in the subset of air forced cooling. A serious challenge in the air forced cooling is to determine the force convection coefficient from the cooling surface, as the accuracy of this coefficient has a direct effect on the accuracy of the temperature prediction of any thermal model. Many practical applications consist of a flat plate with unheated starting sections [7]. Accordingly, we consider determining the heat transfer coefficient over this type of surface using wind tunnel cooling technology. The study is carried out analytically and experimentally.

## II. EMPIRICAL CORRELATIONS

Depending on fluid flow, the forced convection is classified into two categories: external and internal forced convection [7], [5].

### A. External Forced Convection

In the external forced convection, the flow boundary layers develop without any physical limitation, e.g., the fluid flow over a flat plate [7], [5]. As our objective is to consider the heat transfer over the flat plate surface, we will consider various empirical correlations for this problem.

For analytical calculation, the heat transfer coefficient is calculated by empirical correlation. In these correlations, the forced convection coefficient is calculated based on fluid dynamics dimensionless numbers such as Reynolds number (Re), Prandtl number (Pr) and Nusselt number (Nu) [7], [5]. Furthermore, the fluid mode, which can be either laminar or turbulent, is determined by the Reynolds number [8].

For the external type, the Prandtl and Reynolds numbers are determined respectively as [8]:

$$\text{Pr} = c_p \cdot \mu / k, \quad (1)$$

$$\text{Re} = \rho \cdot v \cdot L / \mu, \quad (2)$$

\* Corresponding author.  
E-mail: payam.shams@ttu.ee

where  $c_p$  is the fluid specific heat capacity kJ/(kg°C),  $\mu$  is the fluid dynamic viscosity kg/(m·s),  $k$  is the fluid thermal conductivity W/(m°C),  $\rho$  is the fluid density kg/m<sup>3</sup>,  $v$  is the fluid velocity m/s and  $L$  is the characteristic length of the cooling surface m [8].

According to [9], there are various empirical correlations for forced heat transfer over the flat plate. However, the well-known correlations used to calculate the value of the Nusselt number for an isothermal flat plate in the laminar and turbulent mode are respectively:

$$\text{Nu} = 0.664\text{Re}^{0.5}\text{Pr}^{1/3}, \quad (3)$$

$$\text{Nu} = (0.037\text{Re}^{0.8} - A) \cdot \text{Pr}^{1/3}, \quad (4)$$

where  $A$  is the constant determined by the critical Reynolds number ( $\text{Re}_{Xc}$ ) [5].

$$A = 0.037\text{Re}_{Xc}^{0.8} - 0.664\text{Re}_{Xc}^{0.5}, \quad (5)$$

In cases where the length ( $Xc$ ) over which the transition from laminar to turbulent flow occurs is smaller than the characteristic length ( $Xc/L > 0.95$ ), the Nusselt number is calculated as:

$$\text{Nu} = 0.037\text{Re}^{0.8}\text{Pr}^{1/3}. \quad (6)$$

Finally, the forced convection coefficient ( $h$ ) is calculated as [8]:

$$h = \text{Nu} \cdot k/L. \quad (7)$$

So far, we have considered situations where the entire plate is heated over the whole length. As mentioned, in many situations the flat plates involve an unheated part  $0 < x < \zeta$ , as shown in Fig. 1. This part consists of insulating materials, and there is no heat generation. In this case, the velocity boundary layer starts to develop from  $x = 0$ , but the thermal boundary layer starts to develop from  $x = \zeta$  [7], [10].

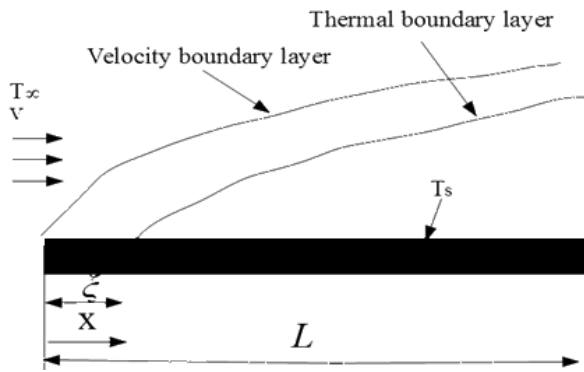


Fig. 1. Illustration of the coolant flows over a flat plate with an unheated part.

The local Nusselt number for this situation under laminar and turbulent modes is respectively calculated as [7]:

$$\text{Nu}_x = \frac{0.332 \text{Re}_x^{0.5} \text{Pr}^{1/3}}{\left[1 - \left(\frac{\zeta}{x}\right)^{3/4}\right]^{1/3}}, \quad (8)$$

$$\text{Nu}_x = \frac{0.0296 \text{Re}_x^{0.8} \text{Pr}^{1/3}}{\left[1 - \left(\frac{\zeta}{x}\right)^{9/10}\right]^{1/9}}, \quad (9)$$

(10) and (11) are applied to calculate the average forced convection coefficient over the flat plate with an unheated part for the laminar and turbulent modes respectively.

$$h = 2 \cdot \frac{1 - \left(\frac{\zeta}{L}\right)^{3/4}}{1 - \left(\frac{\zeta}{L}\right)} \cdot h_{x=L}, \quad (10)$$

$$h = 1.25 \cdot \frac{1 - \left(\frac{\zeta}{L}\right)^{9/10}}{1 - \left(\frac{\zeta}{L}\right)} \cdot h_{x=L}. \quad (11)$$

### B. Internal Forced Convection

In the internal forced convection, the fluid flows inside a confined space, e.g., a cylinder, tube or duct. In this case, the coolant fluid is completely bounded by the inner surface, and the boundary layer cannot expand freely [7], [5]. In this situation, the Reynolds number is defined as:

$$\text{Re} = vD/\vartheta, \quad (12)$$

where  $D$  is the hydraulic diameter of the internal flow, m and  $\vartheta$  is the kinematic viscosity of the fluid, m<sup>2</sup>/s [7].

In the internal forced convection, the laminar and turbulent modes of flow are determined by the Reynolds number too. In this manner, to determine the laminar and turbulent modes of flow, the range of  $\text{Re}$  is defined as [7], [5]:

$$\begin{cases} \text{Re} < 2300 & \text{laminar mode} \\ 2300 \leq \text{Re} \leq 10^4 & \text{transient mode} \\ \text{Re} > 10^4 & \text{turbulent mode} \end{cases}$$

### III. EXPERIMENTAL SETUP

The first objective of the experimental work reflected in this paper is to assess the forced convection heat transfer from the flat side of the coil module with different airflow speeds. The second objective is to compare the analytical data with the experimental data to verify the accuracy of these correlations.



Fig. 2. The coil module used in the experimental work.

As specified in the previous research [1] and [11], the stator coil used in this investigation consists of six different faces, as shown in Fig. 2. To consider the forced convection from the flat side, the heat flux flow should be confined only to the flat side. To achieve this, we created an insulation box according to the dimensions of the coil using foam insulation boards with a thickness of 10 cm. Fig. 3 shows the coil box and the flat side of the coil. Since the foam insulation material has low thermal conductivity  $k = 0.3 \text{ W}/(\text{m}\cdot\text{K})$ , the thermal flux flow is restricted to the open surface. Therefore, the box is operating as a closed calorimeter. Another important point about the box is the temperature operation point; as the foam insulation board can handle temperatures up to  $90 \text{ }^\circ\text{C}$ , during the experiment, the coil temperature should not exceed that temperature.

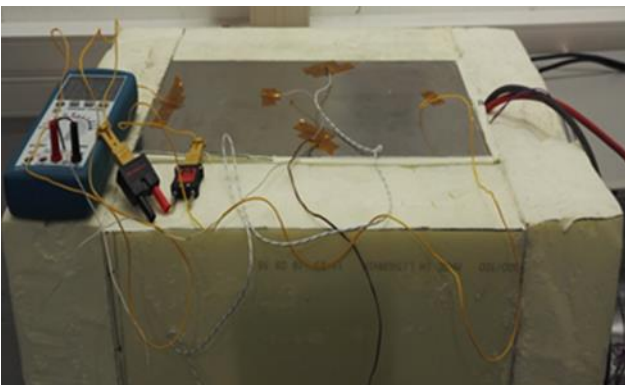


Fig. 3. The used configuration for the flat plate experiment.

The experimental setup for considering the forced convection over the flat side of the stator coil is depicted in Fig. 4. A wind tunnel is constructed of a cylindrical steel pipe with the length of 300 cm and the diameter of 80 cm. A four pole 7.5 kW squirrel cage induction motor is connected to the fan blades as the fan section. It is placed in front of the wind tunnel to blow the air through the tunnel and provide airflow in different speed ranges. The induction motor is controlled with a frequency converter to regulate the coolant flow.

Further, the coil insulation box is used as a calorimeter, and a DC power source is used to heat the coil. The system is protected with the temperature controller sensor to limit the temperature to  $90 \text{ }^\circ\text{C}$ . In addition, the airflow velocity is measured by hot wire anemometer.

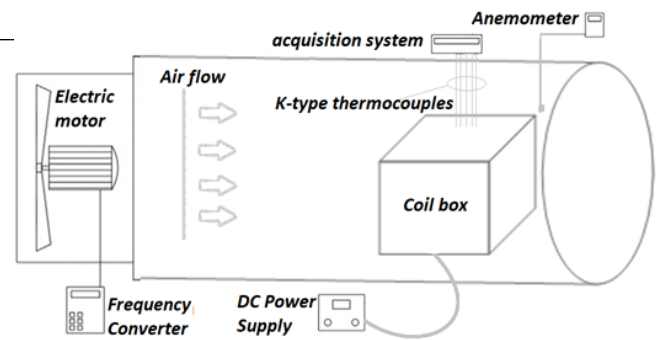


Fig. 4. Schematic diagram of the main part of the experimental setup.

The flat side of the coil module is constructed from stainless steel with a thermal conductivity of  $17 \text{ W}/(\text{m}\cdot\text{K})$  and emissivity of 0.5. The test bench is designed to measure the forced convection coefficient from the flat side of the coil module. For this purpose, we use the DC test method. The DC test is a common experimental method for determining the convection coefficient heat transfer. In the test, the loss of the stator coil is confined to joule loss of the coil winding, and the amount of power can be easily calculated from the measured electric quantities. In the calculations, we accounted for the variations in the winding electrical resistance, as the winding resistivity is temperature dependent [1] and [12].



Fig. 5. Coil box inside the wind tunnel and location of the thermocouples.

During the experiments, the coil module is supplied through a digitally-controlled DC power supply. The voltage and the current are measured to determine the input power, which equals to the heat power. According to Fig. 5, five K-type thermocouples are installed using adhesive material in various locations on the flat side of the coil module. The ambient temperature is also measured using a K-type thermocouple. To increase the accuracy of the temperature measurement and to minimize the contact resistance between the thermocouple and the coil module surface, we used a commercial thermal paste. The average temperature of these five thermocouples is assumed the mean temperature of the flat side of the coil module. During the experiments, all temperature data are collected using a Graphtec GL200 logger. The experiment has been carried out for each airflow speed until the system reached its steady state condition.

## IV. THE ANALYSIS METHOD OF EXPERIMENTAL DATA

The total heat produced in the coil is equal to the total input power. Thus, the total heat is defined as:

$$Q_T = V \cdot I, \quad (13)$$

where

$Q_T$  is the total heat in watts, W;

$V$  is the input voltage in volts, V;

$I$  is the input current in amperes, A.

Accordingly, the total heat is extracted using forced convection and radiation phenomena. Thus, the total heat can be described as:

$$Q_T = Q_c + Q_r, \quad (14)$$

where  $Q_c$  is the amount of heat extracted by forced convection and  $Q_r$  is the amount of heat removed by radiation.

According to [13] and [14], the heat extraction coefficient is calculated as:

$$h_c = Q_T \cdot A^{-1} (T_s - T_a)^{-1}, \quad (15)$$

where  $T_s$  (°C) is the mean temperature of the fin side of the coil module,  $T_a$  (°C) is the ambient temperature and  $A$  (m<sup>2</sup>) is the surface area.

The total heat extraction coefficient is defined as the sum of convection coefficient  $h_c$  and radiation coefficient  $h_r$  [15]. Accordingly, the forced convection coefficient is calculated as:

$$h_c = h_c - h_r. \quad (16)$$

The radiation coefficient is calculated analytically by the following correlation:

$$h_r = \varepsilon \sigma_c (T_s + T_a) (T_s^2 + T_a^2), \quad (17)$$

where  $\varepsilon$  is the emissivity coefficient, and  $\sigma_c$  is the Stefan-Boltzmann constant  $\sigma_c = 5.67 \cdot 10^{-8}$  W/(m<sup>2</sup>K<sup>4</sup>) [14].

## A. Uncertainty Analysis of Experimental Results

In this section, we determined the total accuracy of experimental data according to the accuracy of the measurement instruments. During the experiment, the voltage and current are measured with the TTI QPX1200S. The accuracies of the voltage and current readings are 0.1 % and 0.3 %, respectively. Furthermore, the standard accuracy of the K-type thermocouple is 0.75 %. According to [16], power uncertainty is evaluated as:

$$\omega_{Q_T} = \left[ \left( \frac{\partial Q_T}{\partial V} \cdot \omega_V \right)^2 + \left( \frac{\partial Q_T}{\partial I} \cdot \omega_I \right)^2 \right]^{0.5}, \quad (18)$$

where  $\omega_{Q_T}$ ,  $\omega_V$  and  $\omega_I$  are the uncertainties in the total input power, voltage and current.

This leads to the uncertainty for the computed convection coefficient expressed as:

$$\omega_h = \left[ \left( \frac{\partial h}{\partial Q_T} \cdot \omega_{Q_T} \right)^2 + 2 \cdot \left( \frac{\partial h}{\partial T} \cdot \omega_T \right)^2 \right]^{0.5}, \quad (19)$$

where  $\omega_T$  is the uncertainty in the temperature measurement.

Also, the accuracy of the anemometer for measured speed is  $\pm 3$  % of reading value.

## V. RESULTS &amp; DISCUSSION

The investigations were carried out analytically and experimentally to determine the forced convection coefficient over the flat side of the coil, which is located inside the wind tunnel.

Table I shows experimental data for the case study under fixed current equal to 28 A with different airflow speeds. The total heat extraction coefficients were calculated by using (15). Also, the radiation coefficients were calculated analytically by using (17). Finally, the forced convection coefficients were calculated based on (16).

TABLE I  
EXPERIMENTAL RESULTS

V m/s	T <sub>s</sub> °C	T <sub>a</sub> °C	P <sub>loss</sub> W	h <sub>c</sub> W/(m <sup>2</sup> C)	h <sub>r</sub> W/(m <sup>2</sup> C)	h <sub>c</sub> W/(m <sup>2</sup> C)
4.1	62.7	18.6	137.4	33.70	4.22	29.48
6.1	52.4	18.5	133.0	42.36	4.01	38.36
7.1	50.5	18.7	131.7	44.80	3.97	40.83
8.2	47.2	18.3	130.2	48.96	3.90	45.05
10.5	43.5	18.3	128.4	55.09	3.83	51.26

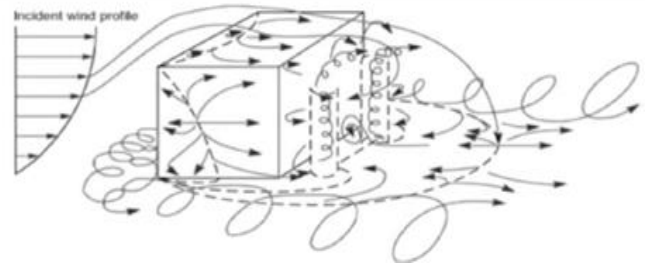


Fig. 6. 3-D wind flow around the rectangular box [17].

In the analytical calculation, as the coil box is located inside the wind tunnel, its boundary layer cannot develop as in the free stream mode. In this situation, the characteristic of the wind tunnel directly affects the fluid flow mode over the plate. According to Fig. 5, the coil box is in the outlet of the wind tunnel, and the turbulent and transition mode occur away from the entrance of the tunnel [18]. Further, as Fig. 6 illustrates, the coil box itself accelerates the wind speed and increases the turbulent situation. Accordingly, the critical Reynolds number for our case study is defined based on the critical Reynolds number in the internal flow. As a result, the fluid flow is in the turbulent mode.

Table II shows the analytical calculation based on the mentioned correlations for forced convection coefficient over the flat plate with the unheated part with a combination of external and internal forced convection modes.

TABLE II

ANALYTICAL RESULTS BASED ON THE COMBINATION OF EXTERNAL AND INTERNAL FORCED CONVECTION

$V$ m/s	$T_s$ °C	$T_a$ °C	$h_{eT}$ W/(m <sup>2</sup> C)
4.1	63	18.0	21.95
6.1	52	18.0	30.63
7.1	50	18.0	34.65
8.2	47	18.0	42.01
10.5	43	18.0	46.15

At the same time, Table III shows the analytical results based on the external forced convection flow mode calculation.

TABLE III

ANALYTICAL RESULTS BASED ON EXTERNAL FORCED CONVECTION FLOW MODE BOUNDARY (LAMINAR MODE)

$V$ m/s	$T_s$ °C	$T_a$ °C	$h_{eL}$ W/(m <sup>2</sup> C)
4.1	63	18.0	13.94
6.1	52	18.0	17.07
7.1	50	18.0	18.42
8.2	47	18.0	19.82
10.5	43	18.0	22.45

As Fig. 5 shows, the flat plate has been started by unheated part with the specification of  $\xi = 0.1$  m and  $L = 0.32$  m. Tables II and III show the analytical data for turbulent ( $h_{eT}$ ) and laminar ( $h_{eL}$ ) modes, the analytical values of which are calculated by using (10), (11) in different wind speed ranges.

Fig. 7 shows the variations of the forced convection heat transfer via the airflow speed based on experimental and analytical data. From the graph in Fig. 7, it is apparent that the convection coefficient heat transfer is proportional to wind speed and it will increase by increasing the speed. Accordingly, the graph proves the importance of accurate comprehensive measurement of fluid flow mode during forced convection heat transfer calculation. As expected, the fluid flow was in the turbulent mode. The linear correlation between the convection coefficient and wind speed is one interesting analytical data-based finding. Another important finding is that the convection coefficient at zero speed is not zero, which can be attributed to the natural convection. Fig. 7 shows that by increasing the wind speed, the experimental data converge toward turbulent analytical results. Thus, it can be expected that the precision of analytical calculations is enhanced at high wind speed with high turbulent flow. However, in forced convection coefficient calculation, 15 % difference between the analytical and experimental data is an acceptable relative difference [5].

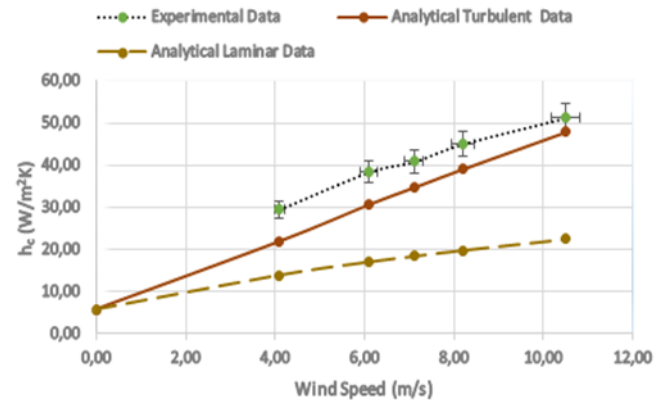


Fig. 7. Convection heat transfer coefficient according to wind speeds.

## VI. CONCLUSIONS

The focus in this paper was made on the determination of the forced convection heat transfer over a flat plate with an unheated part, which is located inside a wind tunnel using analytical and experimental methods. For this purpose, the empirical correlations for internal and external forced convection were studied in detail. Finally, the forced convection coefficients were calculated according to the airflow mode and validated through an experimental test setup. The experimental data were collected for five different airflow speeds.

Considering the results of this study, it can be concluded that the coil's box is generally operated in the turbulent flow. Further, according to analytical results, forced convection has a linear correlation with speed, and it starts to increase by increasing the speed. However, the analytical calculation shows a great precision at the high turbulent flow, but the accuracy decreases at low turbulence.

## REFERENCES

- [1] P. S. Ghahfarokhi, A. Kallaste, A. Belahcen, T. Vaimann, and A. Rassolkin, "Determination of Forced Convection Coefficient Over a Flat Side of Coil," in *58th International Scientific Conference on Power and Electrical Engineering of Riga Technical University (RTUCON)*, 2017, pp. 1–4. <https://doi.org/10.1109/RTUCON.2017.8124759>
- [2] H.-T. Chen, S.-T. Lai, and L.-Y. Haung, "Investigation of heat transfer characteristics in plate-fin heat sink," *Appl. Therm. Eng.*, vol. 50, no. 1, pp. 352–360, Jan. 2013. <https://doi.org/10.1016/j.applthermaleng.2012.08.040>
- [3] P. S. Ghahfarokhi, A. Kallaste, A. Belahcen, and T. Vaimann, "Thermal analysis of electromagnetic levitation coil," in *17th International Scientific Conference on Electric Power Engineering (EPE)*, 2016, pp. 1–5. <https://doi.org/10.1109/EPE.2016.7521725>
- [4] P. S. Ghahfarokhi, A. Kallaste, A. Belahcen, T. Vaimann, and A. Rassolkin, "Review of thermal analysis of permanent magnet assisted synchronous reluctance machines," in *2016 Electric Power Quality and Supply Reliability (PQ)*, 2016, pp. 219–224. <https://doi.org/10.1109/PQ.2016.7724116>
- [5] F. P. Incropera, D. P. DeWitt, T. L. Bergman, and A. S. Lavine, *Fundamentals of Heat and Mass Transfer*, 2007.
- [6] M. Rosu et al., *Multiphysics Simulation by Design for Electrical Machines, Power Electronics, and Drives*, 1<sup>st</sup> ed. Wiley-IEEE Press, 2017. <https://doi.org/10.1002/9781119103462>
- [7] Y. A. Cengel, *Heat Transfer: A Practical Approach*. New York: McGraw-Hill, 2004.

- [8] D. A. Staton and A. Cavagnino, "Convection Heat Transfer and Flow Calculations Suitable for Electric Machines Thermal Models," *IEEE Trans. Ind. Electron.*, vol. 55, no. 10, pp. 3509–3516, Oct. 2008. <https://doi.org/10.1109/TIE.2008.922604>
- [9] E. Sartori, "Convection coefficient equations for forced air flow over flat surfaces," *Sol. Energy*, vol. 80, no. 9, pp. 1063–1071, 2006. <https://doi.org/10.1016/j.solener.2005.11.001>
- [10] F. Kreith and D. Goswami, Eds., *The CRC Handbook of Mechanical Engineering*, Second Edition. CRC Press, 2004.
- [11] P. S. Ghahfarokhi, A. Kallaste, T. Vaimann, and A. Belahcen, "Natural convection from flat side's of coil system," in *2018 19th International Scientific Conference on Electric Power Engineering (EPE)*, May 2018, pp. 1–5. <https://doi.org/10.1109/EPE.2018.8395967>
- [12] P. S. Ghahfarokhi, A. Kallaste, T. Vaimann, A. Rassolkin, and A. Belahcen, "Determination of natural convection heat transfer coefficient over the fin side of a coil system," *Int. J. Heat Mass Transf.*, vol. 126, Part A, pp. 677–682, Nov. 2018. <https://doi.org/10.1016/j.ijheatmasstransfer.2018.05.071>
- [13] M. Markovic, L. Saunders, and Y. Perriard, "Determination of the Thermal Convection Coefficient for a Small Electric Motor," in *Conference Record of the 2006 IEEE Industry Applications Conference Forty-First IAS Annual Meeting*, pp. 58–61, 2006. <https://doi.org/10.1109/IAS.2006.256520>
- [14] O. Meksi and A. O. Vargas, "Numerical and experimental determination of external heat transfer coefficient in small TENV electric machines," in *2015 IEEE Energy Conversion Congress and Exposition (ECCE)*, 2015, pp. 2742–2749. <https://doi.org/10.1109/ECCE.2015.7310044>
- [15] P. S. Ghahfarokhi, A. Kallaste, T. Vaimann, A. Rassolkin, and A. Belahcen "Determination of Thermal Convection Coefficient from Coil's Flat Plate Side," in *2017 IEEE 58th International Scientific Conference on Power and Electrical Engineering of Riga Technical University (RTUCon)*, Riga, Latvia, 2017.
- [16] M. Ahmadi, G. Mostafavi, and M. Bahrami, "Natural convection from rectangular interrupted fins," *Int. J. Therm. Sci.*, vol. 82, pp. 62–71, 2014. <https://doi.org/10.1016/j.ijthermalsci.2014.03.016>
- [17] H. G. C. Woo, J. A. Peterka, J. E. Cemak, "Wind Tunnel Measurements in the Wakes of Structures," Fort Collins, CO, United States, 1977.
- [18] S. M. Ghiaasiaan, *Convective Heat and Mass Transfer*. Cambridge University Press, 2011.



**Payam Shams Ghahfarokhi** was born in Iran, in 1986. He received the B.Sc. degree in electrical power engineering from IAUN in 2010, the M.Sc. degree in electrical power engineering from Newcastle University in 2011 and the Ph. D. degree from Tallinn University of Technology. He is currently a researcher at Tallinn University of Technology, Department of Electrical Power Engineering and Mechatronics. He has been the IEEE member since 2017. His main fields of interest are design of permanent magnet electrical machine and

thermal design of electrical machine.

E-mail: Payam.Shams@taltech.ee

ORCID iD: <https://orcid.org/0000-0002-6917-5883>



**Ants Kallaste** received his B.sc., M.sc. and Ph.D. degrees in electrical engineering from Tallinn University of Technology, Estonia, in 2004, 2006 and 2013, respectively. He is currently a senior researcher at Tallinn University of Technology, Department of Electrical Power Engineering and Mechatronics. He is holding the position of Head of Electrical Machines Research Group. He is the member of IEEE and Estonian Society of Moritz Hermann Jacobi.

His main research interest is design of electrical machines.

E-mail: Ants.Kallaste@taltech.ee

ORCID iD: <https://orcid.org/0000-0001-6126-1878>



**Anouar Belahcen** received the B. sc. degree in physics from the University Sidi Mohamed Ben Abdellah, Fes, Morocco, in 1988 and the M. sc. (Tech.) and Doctor (Tech.) degrees from Helsinki University of Technology, Finland, in 1998, and 2004, respectively.

He is the Professor of Electrical Machines at Tallinn University of Technology, Estonia and the Professor of Energy and Power at Aalto University, Finland.

His research interests are modeling of electrical machines, magnetic materials, coupled magnetic

and mechanical problems and magnetostriction.

E-mail: Anouar.Belahcen@taltech.ee

ORCID iD: <https://orcid.org/0000-0003-2154-8692>



**Toomas Vaimann** received his B. sc., M. sc. and Ph. D. degrees in electrical engineering from Tallinn University of Technology, Estonia, in 2007, 2009 and 2014, respectively. He is currently a senior researcher at Tallinn University of Technology, Department of Electrical Power Engineering and Mechatronics. He has been working in several companies as an electrical engineer. He is the member of IEEE, Estonian Society of Moritz Hermann Jacobi and Estonian Society for Electrical Power Engineering.

His main research interest is the diagnostics of electrical machines.

E-mail: Toomas.Vaimann@taltech.ee

ORCID iD: <https://orcid.org/0000-0003-0481-5066>